The CLIQ Quench Protection System Applied to the 16 T FCC-hh Dipole Magnets

Marco Prioli ⬤, Tiina Salmi ⬤, Bernhard Auchmann ⬤, Lorenzo Bortot ⬤, Michal Maciejewski ⬤, Arjan Verweij ⬤,
Barbara Caiffi, Stefania Farinon ⬤, Clement Lorin ⬤, Michel Segreti ⬤,
Alejandro M. Fernandez, and Javier Munilla ⬤

Abstract—Part of the Future Circular Collider (FCC-hh) study is dedicated to the development of the 16 Tesla Nb_3Sn superconducting dipole magnets. The design of the magnets was enabled by a cooperative effort of national research institutes, universities, and CERN. These actors tackled the problem from different sides, namely, the electromagnetic design, the mechanical design, the design of the quench protection systems, and the circuit design. The article deals with the design of the quench protection systems and provides solid motivations for the selection of the coupling-loss-induced quench (CLIQ) device as the baseline protection system for the FCC-hh main dipole magnets. The article shows that the design domains mentioned above are tightly interconnected and, therefore, the simulation of a quench event involves a complex multiphysics problem. The STEAM cosimulation framework, recently developed at CERN, is applied to address the complexity. The STEAM-SIGMA models are employed to simulate the CLIQ quench protection system applied to the FCC-hh dipole magnets. Dedicated CLIQ configurations are identified to protect the magnets in case of a quench. In addition, the possible implications of the CLIQ protection system on the mechanical design of the magnets are discussed. To this end, the article employs the co-simulation of different software platforms to calculate the mechanical stress during a quench. The results show that CLIQ does not produce additional stress.

M. Prioli is with Machine Protection and Electrical Integrity Group, Technology Department, CERN, 1211 Geneva, Switzerland. He is now with the National Institute for Nuclear Physics (INFN)–LASA, 20090, Segrate (MI), Italy (e-mail: marco.prioli@mi.infn.it).

T. Salmi is with the Tampere University of Technology, 33101 Tampere, Finland.

B. Auchmann is with Machine Protection and Electrical Integrity Group, Technology Department, CERN, 1211 Geneva, Switzerland, and also with the Paul Scherrer Institute, 5232 Villigen, Switzerland.

L. Bortot and A. Verweij are with Machine Protection and Electrical Integrity Group, Technology Department, CERN, 1211 Geneva, Switzerland.

M. Maciejewski is with Machine Protection and Electrical Integrity Group, Technology Department, CERN, 1211 Geneva, Switzerland, and also with the Łódź University of Technology, 90-924 Łódź, Poland.

B. Caiffi and S. Farinon are with the National Institute for Nuclear Physics (INFN), 16146 Genova, Italy.

C. Lorin and M. Segreti are with the Atomic Energy and Alternative Energies Commission (CEA) Saclay 91191 Gif-sur-Yvette cedex, France.

A. M. Fernandez and J. Munilla are with the Centro de Investigaciones Energéticas, Medioambientales y Tecnológicas (CIEMAT), 28040 Madrid, Spain.

Color versions of one or more of the figures in this article are available online at http://ieeexplore.ieee.org.

Digital Object Identifier 10.1109/TASC.2019.2930705

I. INTRODUCTION

A 100 TeV, 100 km proton–proton circular collider is under study for the Future Circular Collider (FCC) project [1]. One of the actors involved is EuroCirCol, the European Circular energy-frontier Collider study, whose work package 5 is dedicated to the design of 16 Tesla Nb_3Sn superconducting dipole magnets [2], [3]. Three different options were originally taken into consideration for the magnet design, namely, the cos-θ [4], block coil [5], and common coil [6] type cross sections. Later, a canted cos-θ magnet [7] was added as the fourth option.

Fig. 1 summarizes the different domains considered during the design of each magnet, namely, the electromagnetic design, the mechanical design, the design of the quench protection systems, and the circuit design. The electromagnetic and mechanical designs are carried out by four different laboratories, one for each magnet design, and are discussed in [4]–[7]. On the other hand, the quench protection analysis is centralized for all options except for the canted cos-θ since its simulation requires dedicated three-dimensional models and is therefore performed by the institute that is also responsible for the electromagnetic and mechanical design [7]. The fourth aspect considered is the study of the layout of the circuit containing the FCC magnets and it is also centralized. This last aspect is discussed in the companion paper [8].

Due to the tight coupling among the considered domains, many iteration loops are needed to reach the final magnet design. As an example, the study of the quench protection systems is needed to assess the *protectability* of a given magnet design. If the analysis shows that no system can protect the magnet in case of a quench, this produces a feedback on the electromagnetic design, which has to be reiterated to match the *protectability* requirement. According to EuroCirCol specifications [2], [3], a magnet is considered protected when the adiabatic hotspot temperature and voltage-to-ground developed during a quench do not exceed 350 K and 1.2 kV, respectively. The time to detect and validate the quench is assumed to be 20 ms.

This requirement was initially verified by means of a simplified approach [9] which assumed that the entire superconducting coil can be uniformly quenched 40 ms after an initial quench transition and considered adiabatic conditions for the calculation of temperature rise. Later, the analysis considered
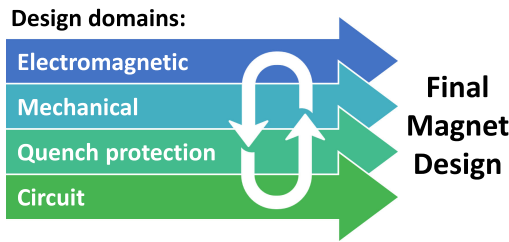
Fig. 1.   Domains considered during the design of the FCC 16 T superconducting dipole magnets.

actual quench protection systems. Two different options were explored for the 16 T magnets: the quench heaters (QH) [10] and the coupling-loss-induced quench (CLIQ) system [11], [12]. The quench heater design is already addressed in [9], [13], [14]. The aim of this article is to present the final CLIQ protection schemes and demonstrate that this technology can protect the cos-θ, block coil, and common coil magnets in case of a quench.

Another example of the coupling is the one between the electromagnetic design and the circuit design. The electrical insulation of the magnet coils is designed to withstand a maximum voltage-to-ground. Since the electrical circuit contains a large number of dipole magnets, the maximum voltage-to-ground depends on the adopted circuit layout. This aspect is discussed in the companion paper [8]. In this article, another feedback loop of Fig. 1 is described in detail, namely the effect of the quench process on the mechanical domain. A method for the calculation of the mechanical stress during a quench is proposed and employed to assess the effect of the CLIQ protection system from the mechanical point of view. According to the aforementioned EuroCirCol specifications [2], [3], the mechanical design criterion is a maximum stress in the coils of 200 MPa at cold.

II. DIPOLE MAGNETS

Figs. 2–4 depict the geometry of coils and part of the iron yoke of the cos-θ, block coil, and common coil magnets designs, respectively. Labels have been assigned to identify the coil layers. For cos-θ and block coil, the label "R" marks the coils belonging to the right aperture and the label "L" the ones belonging to the left aperture. For the third magnet design, as suggested by its own name, the coils are common to the two apertures.

The magnet parameters can be found in [4]–[6]. We recall here only the main features useful for the analysis developed in this article. The parameters common to the three magnet designs are reported in Table I, while the ones specific to each design are reported in Table II. It is worth noting that the designs are graded, i.e., two different superconducting cables are used: a larger cable for the regions with higher magnetic fields and a smaller one for the regions with a lower field where less superconductor is needed. This technique is adopted to increase the efficiency of the conductor and reduce the total quantity of superconducting material.

III. QUENCH PROTECTION

A. Strategy

After a quench [15] in a 16 T FCC dipole magnet is initiated, an active protection system is needed to spread the initial normal

conducting zone to the largest possible volume of coil in the shortest possible time, limiting at the same time the induced voltages. Almost all the energy stored in the magnet is deposited in its coils. The active protection system affects the distribution of the energy deposition across the coils and, in this way, it can decrease the hotspot temperature and voltage-to-ground developed during a quench.

Two different options were considered for the protection of the FCC dipole magnets. The first one relies on quench heaters, a strategy already adopted for the protection of the dipole magnets of the Large Hadron Collider (LHC) [10]. Quench heaters are metallic strips in thermal contact with the magnet coils through the electrical insulation layer. When a current flows through the strip, heat is deposited due to the Joule effect and propagated to the coils across the electrical insulation. The design of the quench heaters for the FCC magnets is discussed in [9], [13] and shows that all designs can be protected in case of a quench. The main drawback of this solution, when applied to the 16 T magnets, is the high number of required heater powering supplies and heater strips [9], [13].

The second option relies on the CLIQ system [11], [12]. Unlike quench heaters, which consist of an external heat source, CLIQ deposits losses directly into the magnet coils. As shown in Fig. 5, CLIQ is composed of a capacitor bank C charged at a given voltage U_0 and connected to the magnet coils through a switch. When the switch is activated, the CLIQ circuit is closed and oscillating LC currents I_1 and I_2 flow through the magnet coils. These currents induce coupling losses inside the coils [15], [16]. Compared to quench-heaters, whose effectiveness is intrinsically limited by the thermal propagation process, CLIQ is faster in propagating the normal conducting zone after a quench at high operating current [11], which is the most critical regime for the hotspot temperature. Moreover, it is easier to implement the CLIQ system and it is intrinsically a more robust solution than quench-heaters as it mitigates the risk of electrical shorts inside the magnets. These key features explain why CLIQ was considered, from the beginning of the study, as a promising option for the protection of the high energy density FCC magnets.

B. Model

The simulation of a quench in a superconducting magnet belongs to the class of the so-called multithree problems: multiscale due to the different size of the elements to be simulated, multi-rate due to the different time constants of the physical phenomena involved, and multiphysics as it has to consider the electric, magnetic, thermal, and mechanical domains. In order to cope with this complexity, a modular simulation framework called STEAM has been recently proposed [17]–[21]. STEAM stands for Simulation of Transient Effects in Accelerator Magnets and has been developed at CERN also to cover the simulation needs arising from the design of the FCC quench protection systems. The STEAM module used for the quench simulations presented in this article is called SIGMA (STEAM Integrated Generator of Magnet models for Accelerators). SIGMA offers a Java API through which the user can define geometry, material properties, and physical laws of the different parts composing

Fig. 2. Labels assigned to the coil layers of the cos-θ magnet. In the coils, the dominant locations where coupling losses are deposited by adopting the CLIQ connection scheme in Fig. 6(a) are highlighted with red color.
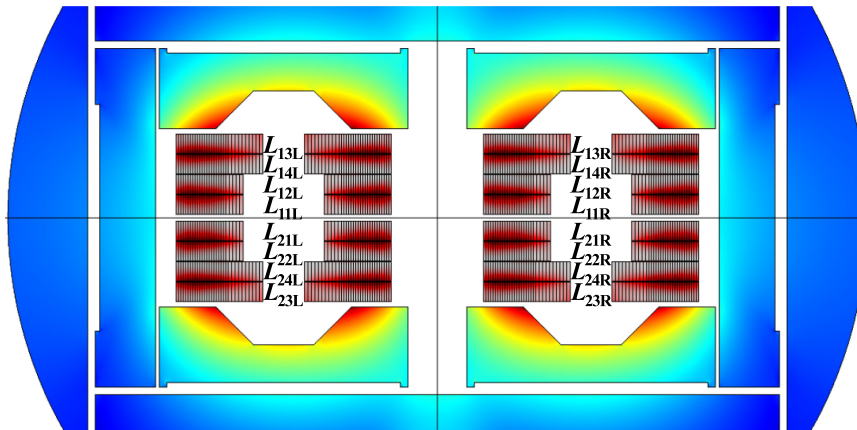
Fig. 3. Labels assigned to the coil layers of the block coil magnet. In the coils, the dominant locations where coupling losses are deposited by adopting the CLIQ connection scheme in Fig. 6(b) are highlighted with red color.
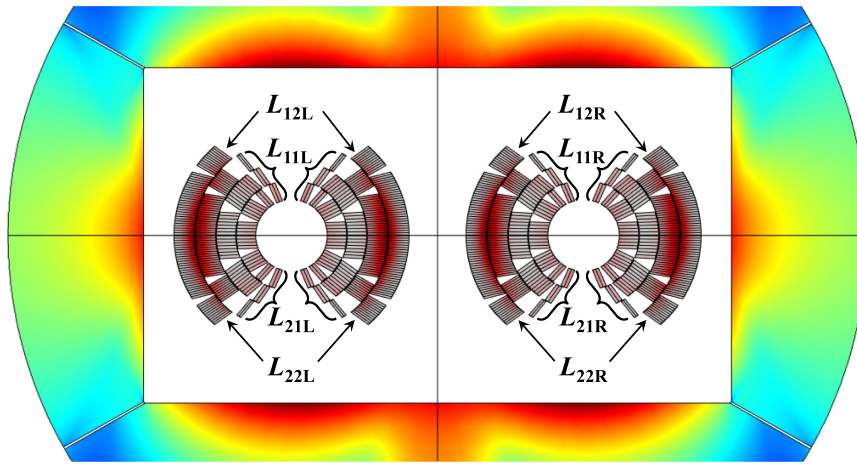

Fig. 4. Labels assigned to the coil layers of the common coil magnet. In the coils, the dominant locations where coupling losses are deposited by adopting the CLIQ connection scheme in Fig. 6(c) are highlighted with red color.
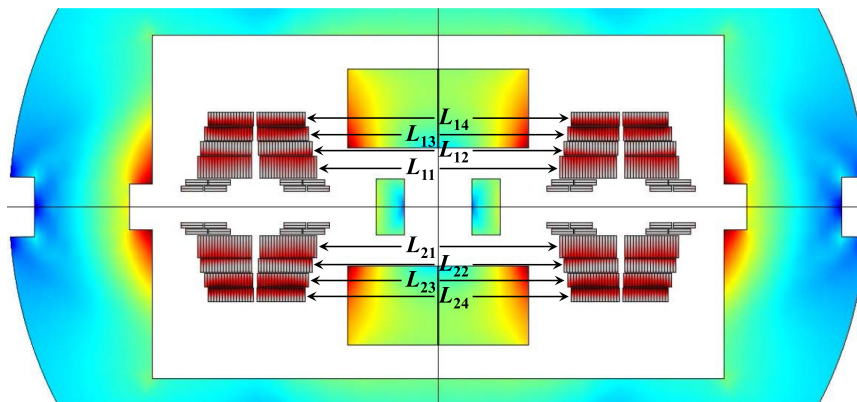
TABLE I
COMMON DIPOLE MAGNETS PARAMETERS

Magnet length (m)	14.3
Cable insulation thickness (glass) (mm)	0.15
Filament twist-pitch (mm)	14
Angle for strand twist-pitch ($^\circ$)	15
Residual-resistivity ratio (RRR)	100

an accelerator magnet. Through a dedicated plug-in, this description is translated into an input file for a numerical tool. For this publication, the tool in question is COMSOL [22]. The COMSOL model thus generated by SIGMA includes, as its key features, the calculation of interfilament and interstrand coupling losses [15], [16] and the simulation of a CLIQ discharge [18].

The SIGMA-generated models cover two requirements specifically related to the simulation of quenches in FCC magnets. The first one, covered by the Java API [21], is the need of *automation* in the construction of the employed numerical models, which is fundamental since different magnet designs, each of them evolving in time, had to be considered. The second one is the need for *predictability* of the simulation results, arising from the impossibility of crosschecking simulations with measurements. The SIGMA-generated COMSOL models cover this requirement through an intrinsically accurate formulation of the electromagnetic and thermal domains based on finite elements [18], [19].

Their inputs are the geometry of coils and iron yoke [3]–[6], the cable parameters (Tables I and II), the material properties (derived from the NIST database), the critical current fit [23], and the characteristics of the CLIQ units (following Table III). Moreover, the matrix resistivity seen by the interfilament coupling currents is assumed to be equal to the copper resistivity. The models do not consider the interstand coupling losses. In the cored FCC cable, their contribution is assumed to be negligible with respect to the interfilament losses due to the relatively high interstrand resistance.

SIGMA-generated models are employed in this article to prove the ability of CLIQ to protect the two-aperture FCC dipole magnets in case of a quench. In order to speed up the exploration of the CLIQ parameters space, faster and simpler numerical models based on the LEDET software [24] and considering the single-aperture versions of the magnet designs were initially employed. The results were presented in [9], [25].

C. Results

Fig. 6 shows equivalent circuits with the CLIQ units and their connection to the windings for the three magnet designs. The circuits are symmetric with respect to the mid-point "M," i.e., the impedance on the left and on the right of this point is the same. This is particularly beneficial for the developed voltage-to-ground. As a consequence, the current I_{a2} flowing in the cos-θ coil layers L_{12} and L_{22} is the same for both apertures. The symmetry applies also to the other magnet designs.

For the cos-θ magnet [Fig. 6(a)], one CLIQ unit per magnet aperture is sufficient to protect the magnet in case of a quench. When it is activated, the current I_{a2} increases (according to the CLIQ current convention shown in the figure) while the current I_{a1} decreases. This unbalance, which consists of an LC oscillatory wave, generates coupling losses that are maximum in the region of the interface between windings with different currents. The distribution of the coupling losses is highlighted with red color in Figs. 2–4. For the cos-θ design, the highest losses are deposited in-between L_{n1} and L_{n2}, where $n = 1, 2$, for both apertures. This CLIQ connection is adopted to quench as fast as possible the outer layers that contribute most to the magnet resistance, due to the relatively low heat capacity [4].

For the block coil magnet, Fig. 6(b) shows the connection scheme only for the left aperture. As for the cos-θ magnet, the circuit of the right aperture is identical to the left one. Two CLIQ units per aperture are needed to protect this magnet. A single CLIQ unit would be sufficient to keep the hotspot temperature below 350 K but the voltage-to-ground developed during a quench would be excessive. The connection of the CLIQ units is optimized in order to deposit coupling losses efficiently and uniformly across the magnet cross section. For the common coil magnet [Fig. 6(c)], two CLIQ units per magnet are needed to protect the magnet in case of a quench, i.e., the same total number of units as for the cos-θ design. Two units are sufficient for the protection, despite the larger coil volume with respect to the other designs. The adopted CLIQ connection scheme is similar to the one of the block coil. Besides the connection schemes, also the charging voltage and capacitance of the CLIQ units are optimized for each magnet design. Their values are reported in Table III.

The currents in the windings of the three magnet designs are shown in Fig. 7. Due to the circuital symmetry, two different currents are obtained for the cos-θ magnet and three for the block coil and common coil magnets. After the CLIQ activation at $t = 0$, the currents show oscillations that are soon damped by the growing magnet resistance resulting from the spread of the normal zone induced by CLIQ. The current decays quasi-exponentially with a time constant of about 0.1 s for all magnet designs. By this time, the majority of the energy originally stored in the magnet is converted into Joule heating in the coils.

The resulting coil temperature at nominal operating current is shown in Fig. 8 and it does not exceed 205 K for all designs. The worst case hotspot temperature is calculated considering adiabatic conditions and a detection and validation time of 20 ms plus 1 ms for the activation of CLIQ. For all designs, the hotspot temperature is close to 280 K, well below the limit of 350 K, thus proving the capability of CLIQ to effectively protect the magnets in case of a quench.

Fig. 9 shows the evolution of the maximum voltage-to-ground during a quench for the three magnet designs. This voltage is due to the unbalance in the distribution of the inductive and resistive voltage over time. The cos-θ and block coil magnets show similar values: the peak voltage of 0.8 kV (cos-θ) and 0.7 kV (block coil) is reached about 120 ms after the activation of CLIQ. For the common coil, the peak voltage-to-ground is 1.1 kV and it is reached later, 165 ms after the activation of the

TABLE II
SPECIFIC DIPOLE MAGNETS PARAMETERS

| Magnet type	cos-θ		Block coil		Common coil	
Nominal current (A)	11390		10111		16400	
Inductance (mH/m)	$2 \cdot 19.8$		$2 \cdot 24.8$		21.1	
Cable type	High-field	Low-field	High-field	Low-field	High-field	Low-field
Cable bare size (mm)	13.2 x 2	14.0 x 1.33	12.6 x 2.0	12.6 x 1.27	19.2 x 2.2	12.0 x 2.2
Number of strands	22	38	21	34	30	18
Strand diameter (mm)	1.1	0.7	1.1	0.7	1.2	1.2
Copper Nb_3Sn ratio	0.82	2.1	0.8	2.0	1.0	2.5
Strand pitch-length (mm)	90	100	85	88	135	85
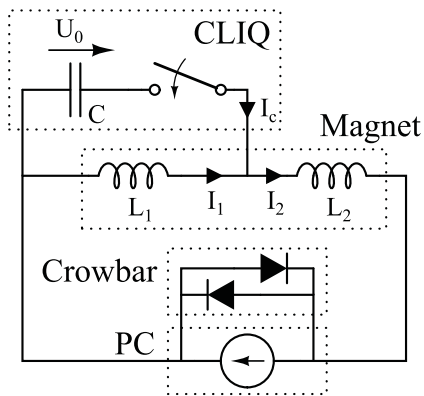
Fig. 5. Circuit schematic showing the CLIQ unit connected to a magnet. The power converter (PC) and its crowbar are also shown.

TABLE III
VOLTAGE AND CAPACITANCE OF THE CLIQ UNITS

	CLIQ1 (L and R)	CLIQ2 (L and R)
cos-θ	1.25 kV – 50 mF	–
block coil	0.6 kV – 50 mF	1.2 kV – 50 mF
common coil	0.9 kV – 50 mF	0.9 kV – 50 mF

quench protection system. For all magnet designs, the identified CLIQ configuration ensures that the peak value of the voltage-to-ground is lower than the considered limit of 1.2 kV.

The distribution of the voltage-to-ground in the coils at the moment of its peak is shown in Fig. 10. For the cos-θ magnet, the maximum turn-to-turn voltage is 70 V and the maximum layer-to-layer voltage is 1.2 kV and it is located between layers L_{11} and L_{12} (see Fig. 2) on the left side of the coils. It can be noticed that the voltage-to-ground is not fully symmetric in the left and right sides, e.g., its minimum value of -400 V is located on the left side. As shown in Fig. 2, the two magnet apertures are housed in a common iron yoke. In this configuration, the yoke is not symmetric with respect to the center of one aperture and a slight asymmetry in the voltage distribution is obtained. For the block coil magnet, the maximum turn-to-turn voltage is 65 V and the maximum layer-to-layer voltage is 1 kV and it is located between layers L_{13} and L_{14} (see Fig. 3) on the right side of the coils. Finally, for the common coil magnet, the maximum

turn-to-turn voltage is 85 V and the maximum layer-to-layer voltage is 1.1 kV and it is located between layer L_{11} and the ancillary coils (see Fig. 4) on the right side of the coils. These values, summarized in Table IV, do not unveil any potential issues for the electrical insulation of the coils with respect to the parameters considered during the electromagnetic design.

Finally, the effectiveness of the CLIQ protection system was checked also at low current values. All magnet designs are protected in case a quench occurs down to operating currents as small as 1 kA.

D. Expected Uncertainty

The results presented in the previous section were compared with the ones obtained through the alternative simulation software LEDET [24]. The difference of the simulated hotspot temperatures is less than 10 K, and the variation of the maximum voltage-to-ground is at most 100 V. These numbers give an indication of the possible model uncertainty. However, it is worth noting that part of the difference is also due to the fact that single-aperture magnets are simulated in LEDET while the complete two-aperture designs are considered in the SIGMA-generated models.

Another possible source of uncertainty lies in the input parameters. Simulations were performed in LEDET considering a possible variation of the cable RRR from 50 to 200 (nominal 100) and the filament twist pitch from 10 to 20 mm (nominal 14 mm). Moreover, the scaling factor which multiplies the copper resistivity to find the matrix transverse resistivity seen by the interfilament coupling currents was varied from 0.5 to 2 (nominal 1). The difference from the reference case is less than 20 K for the hotspot temperature and 250 V for the voltage-to-ground in all cases.

IV. MECHANICAL STRESS DURING QUENCH

A. Strategy

The previous section showed that a quench protection system based on two CLIQ units for the cos-θ and common coil magnets and four units for the block coil magnet provides an effective protection in case of quench as it ensures that the hotspot temperature and voltage-to-ground remain within the considered limits. However, this analysis is partial as it considers only two of the
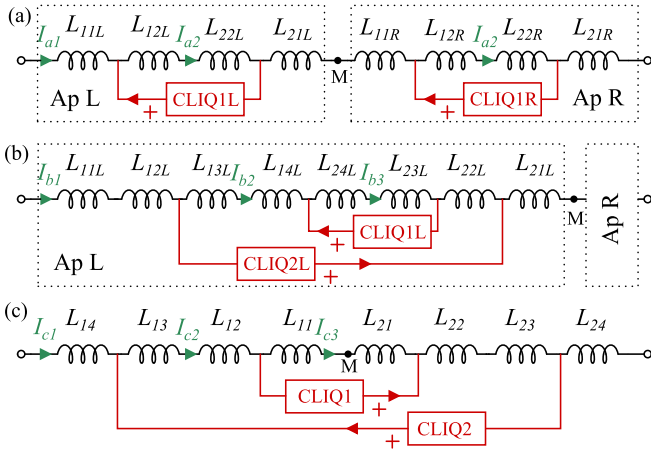
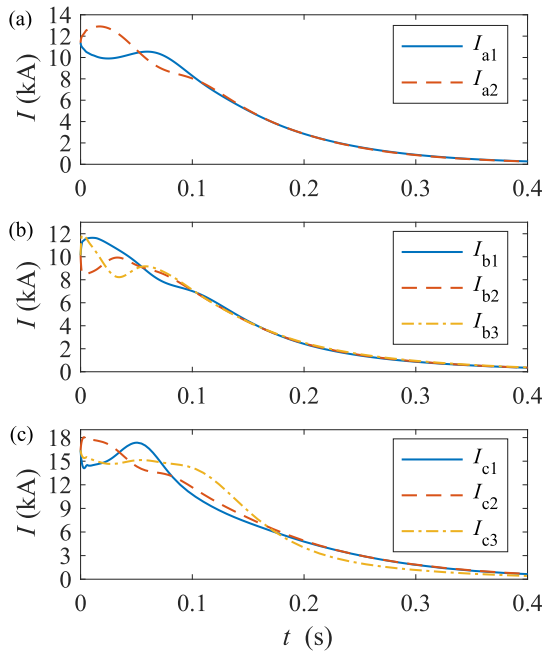Fig. 6. Adopted CLIQ connection scheme for (a) cos-θ, (b) block coil, and (c) common coil designs.

Fig. 7. Currents in the coils during the CLIQ discharge for (a) cos-θ, (b) block coil, and (c) common coil designs.

Fig. 8. Distribution of the final temperature in the coils after a quench for (a) cos-θ, (b) block coil, and (c) common coil designs. The location and value of the adiabatic hotspot temperature (HST) is also shown.

Fig. 9. Maximum absolute value of the voltage-to-ground during a quench for the three magnet designs. Markers identify its peak values.

four design domains identified in Fig. 1, namely the thermal and the electromagnetic domains. For an exhaustive study, one must also consider the possible implications of the CLIQ protection system on the other two domains. The potential issues introduced by CLIQ at the circuital level are discussed in the companion paper [8], which shows that CLIQ is not adding complexity to the circuit design. The potential issues introduced by CLIQ at the mechanical level, in terms of additional mechanical stress with respect to the one predicted by the standard mechanical analysis, need to be carefully evaluated.

The activation of CLIQ results in different currents in the magnet windings due to the injected CLIQ current. If the non-linear effects introduced by the iron yoke are neglected, the total Lorentz force seen by the windings is the sum of the contribution
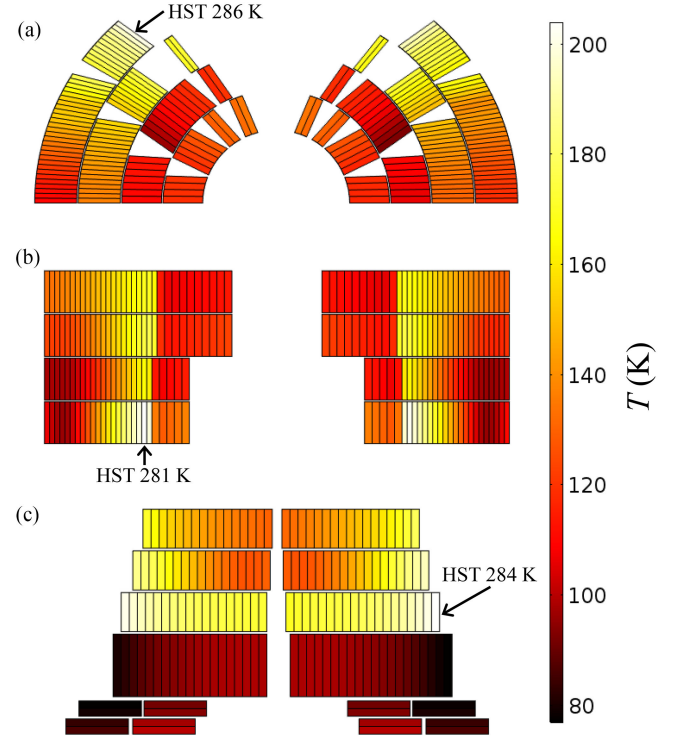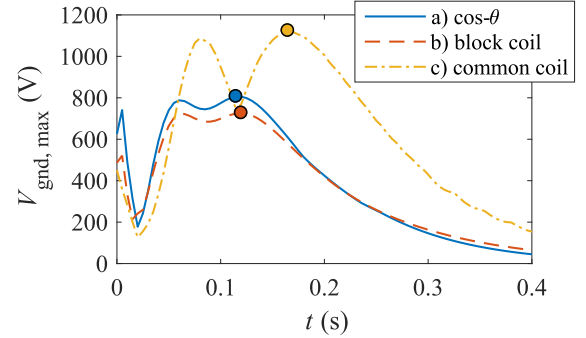
of the nominal transport current and the contribution of the CLIQ current, which generates a magnetic field different from the dipole. Even with iron yoke saturation, one can conclude that the CLIQ current affects the intensity and direction of the total Lorentz force and this aspect is not considered in the mechanical design. The second discrepancy with respect to the standard mechanical analysis is the presence of significant temperature differences in the windings generated by the quench process, which produce a thermal strain and affect the mechanical stress. For these reasons, it is worth to calculate the mechanical stress considering the evolution of the Lorentz force and temperature distributions after a quench and check whether the EuroCirCol design criterion of 200 MPa for the maximum stress at cold is still fulfilled.
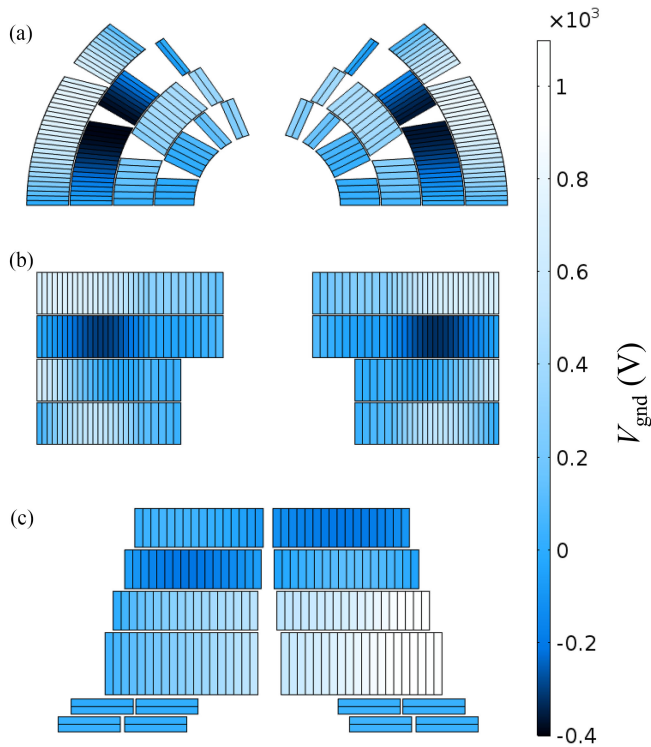
Fig. 10. Distribution of the voltage-to-ground in the coils at the moment of its peak (see markers in Fig. 9). (a) cos-θ design ($t_{peak} = 0.115$ s), (b) block coil design ($t_{peak} = 0.12$ s), and c) common coil design ($t_{peak} = 0.165$ s).

Fig. 11. Temperature-dependent nonlinear thermal strain function in the x and y directions.

TABLE IV
PEAK VOLTAGES AFTER A QUENCH IN THE FCC DIPOLE MAGNETS

	Voltage-to-ground (kV)	Layer-to-layer voltage (kV)	Turn-to-turn voltage (V)
cos-θ	0.8	1.2	70
block coil	0.7	1	65
common coil	1.1	1.1	85

B. Model

As described above, the numerical model for the simulation of the CLIQ protection system considers the electromagnetic and thermal domains and is implemented in COMSOL [22]. On the other hand, the numerical model for the simulation of the mechanical response is implemented in ANSYS [26]. In particular, the mechanical models of the cos-θ and block coil magnets are implemented through ANSYS APDL language, while the model of the common coil is implemented in ANSYS Workbench. The analysis of the mechanical stress developed during a quench requires that the evolution of temperature and Lorentz force in the coils, calculated by means of COMSOL, are imported into ANSYS mechanical models. The main challenge lies in the different mesh employed in the two finite elements solvers, which implies that an interpolation technique has to be adopted to import the mesh-dependent quantities.

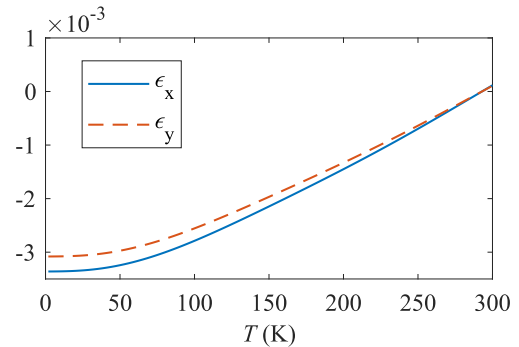One possibility to overcome the interpolation is proposed in [27] where the APDL models of the cos-θ and block coil magnets are translated into equivalent mechanical models in COMSOL. In this article, a different strategy is applied in order to fully profit from existing numerical models. A mesh-based interpolation technique is applied to perform a cosimulation of COMSOL and ANSYS models [28], by exploiting the capabilities of the commercial software MpCCI [29]. Since MpCCI supports the coupling with ANSYS APDL models but does not support ANSYS Workbench models, this automated technique is applied for the cos-θ and block coil magnets only. For the common coil magnet, a different coupling strategy is applied: the information related to mesh, temperature, and Lorentz force calculated in COMSOL is first exported to a text file. The mechanical simulation is then performed by applying the mesh-based interpolation directly in the ANSYS Workbench model (a task which was carried out by the CIEMAT institute). In both cases, the effectiveness of the coupling technique was verified by comparing the results of the COMSOL-ANSYS cosimulation with the ANSYS monolithic mechanical simulation for the case at nominal operating current (i.e., no CLIQ currents) and nominal temperature (i.e., uniform temperature of 1.9 K in the coils).

Note that [27] considers earlier versions of single-aperture electromagnetic and mechanical designs of only the cos-θ and block coil magnets and also previous configurations of the CLIQ protection. In this article, the final designs are considered, including as well the common coil magnet, along with the optimized CLIQ configurations. Therefore, a direct comparison with the results in [27] is not possible.

Fig. 11 shows the temperature-dependent nonlinear thermal strain function considered as an input of the mechanical models. According to EuroCirCol assumptions [2], [3], the coil is considered as a block of uniform material with thermal strain from 293 to 4.3 K of $-3.36e-3$ and $-3.08e-3$ in the x and y directions, respectively. The x direction is along the cable width and the y direction is along the cable height, following the cable orientation in the block coil magnet (see Fig. 3). The thermal strain function is obtained from measurements on Nb_3Sn cables done at CERN [30], scaled to match EuroCirCol assumptions. Apart from this feature, the employed mechanical models and inputs are the same as in the standard mechanical analysis and are described in [4]–[6].
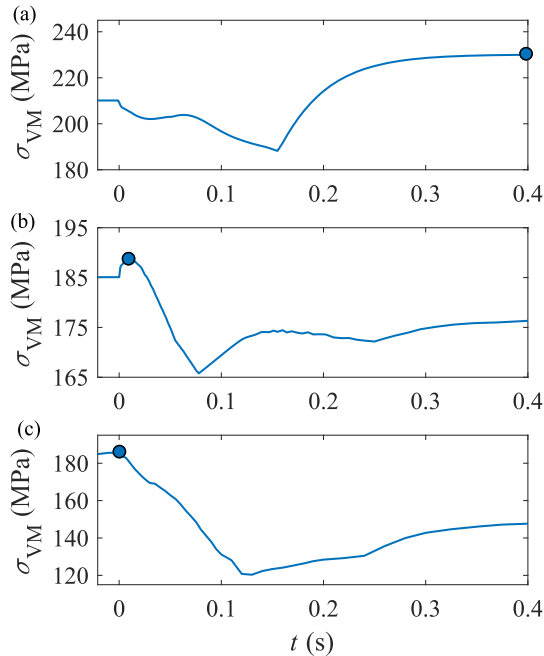
Fig. 12. Maximum Von Mises stress during a quench in the coils of (a) cos-θ, (b) block coil, and (c) common coil designs. Markers identify its peak values.

C. Results

The mechanical stress during a quench is influenced by the location where the resistive transition originated. It was found that the highest stress values are obtained for all magnet designs when the original quench is located in the zone with maximum stress. The following figures correspond to this case.

Fig. 12 shows the maximum Von Mises stress[1] in the coils of the three magnet designs after the CLIQ system is fired at $t = 0$ and the magnets are quenched. At $t < 0$, the peak Von Mises stress corresponds to the one given by the standalone simulation in ANSYS at energization. When CLIQ is fired, the stress shows a different evolution for the three magnet designs. For the cos-θ magnet, the peak stress is initially lowered by the additional Lorentz force introduced by the CLIQ currents and, later, when the transport current is close to zero (see Fig. 7), it is increased by the thermal gradients and the resulting thermal strain developed in the coils (see Fig. 8). The final peak stress is 230 MPa, 20 MPa higher than the value at the energization stage. For the block coil magnet, the evolution of the stress is the opposite: it is initially increased by the additional Lorentz force and later it is reduced by the thermal gradients. The peak stress is actually increased by only 4 MPa with respect to the energization phase. For the common coil magnet, the stress during a quench is always lower than that at the energization stage.

The time and value of the peak stress are highlighted by the blue markers in Fig. 12. The distribution of the Von Mises stress in the coils of the three magnet designs is shown in Fig. 13.

<hr>

[1]Note that the mechanical models consider the coils bonded to the posts, as specified within the EuroCirCol collaboration. This assumption may affect the peak stress at the coil-post interfaces. Nevertheless, the modeling approach is consistent between the models, allowing the comparison.
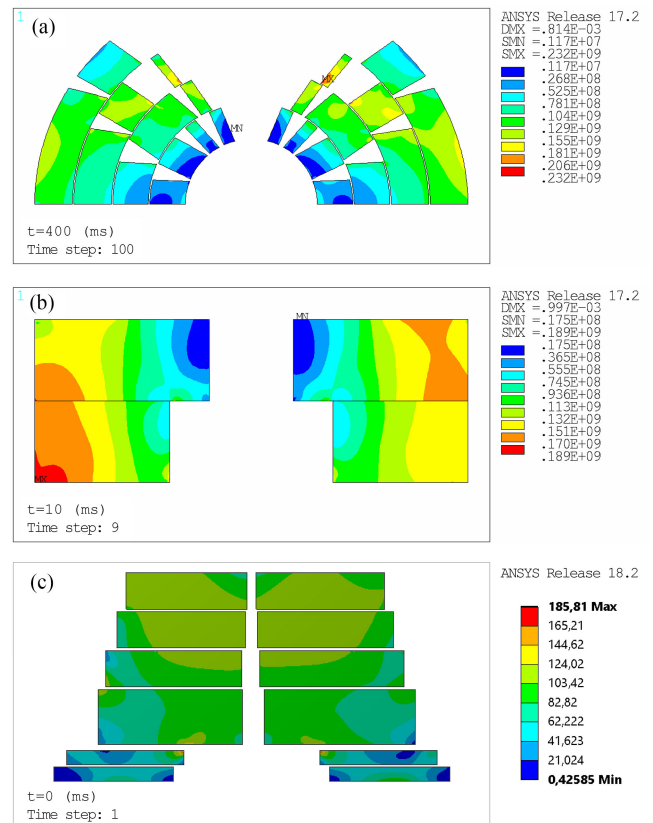

Fig. 13. Distribution of the Von Mises stress in the coils at the moment of its peak (see markers in Fig. 12). (a) cos-θ design ($t_{\mathrm{peak}} = 0.4$ s). (b) Block coil design ($t_{\mathrm{peak}} = 0.01$ s). (c) Common coil design ($t_{\mathrm{peak}} = 0$ s).

It can be seen that for cos-θ magnet, the maximum stress is localized in a small area of the third layer toward the pole. As shown in [4], the same stress distribution appears also after cooldown. The mechanical design is being optimized to reduce the localized peak. For the block coil and common coil magnets, the maximum stress is localized toward the mid-plane and in the ancillary coils, respectively, and its value does not exceed the EuroCirCol specifications of 200 MPa for the maximum stress at cold.

For all three magnet designs, the additional Lorentz force introduced by the operation of the CLIQ system does not significantly increase the stress in the coils. On the other hand, the temperature differences induced by the quench process may increase the stress. It is worth to note that a standard protection system based on quench heaters would lead to similar temperature differences, as shown in [14].

V. CONCLUSION

This article shows that the design of the CLIQ quench protection system is mutually coupled with the other magnet designs steps and requires a dedicated multiphysics approach for its simulation. The STEAM cosimulation framework was applied to address the complexity of the problem. Its features of model automation, model accuracy, and cosimulation of multiple models were essential for the study.

The final configuration of the CLIQ system was proposed for each of the two-apertures FCC dipole magnets designs and its effectiveness to protect the magnets in case of a quench was verified by means of the STEAM-SIGMA electro-thermal magnet models. The simulations show that CLIQ ensures that the maximum hotspot temperature and voltage-to-ground are within the required limits. Moreover, the number of needed CLIQ units is much lower than the number of quench-heater firing units. The fact that magnets can be protected in case of a quench is the result of an iterative approach in which the design of the quench protection systems was integrated with the other design steps.

The potential implications of the CLIQ system on the mechanical design were investigated by means of the STEAM co-simulation framework. A mesh-based interpolation technique was applied to couple the magneto-thermal model, simulating the quench, with the mechanical model. This enabled the possibility of simulating the mechanical stress during a quench. The analysis of the simulation results led to two conclusions. On the one hand, the CLIQ system does not increase the mechanical stress and, therefore, the complexity of the mechanical design is unaltered. On the other hand, the quench process may lead to higher stress than the other operational phases and, for this reason, has to be considered during the mechanical design.

Considering the results reported in the companion paper [8], which show that CLIQ can be employed to protect a string of 16 T magnets, the article makes the CLIQ system a strong candidate for the protection of the FCC-hh main dipole magnets.

REFERENCES

[1] FCC Website. Accessed: Oct. 1, 2019. [Online]. Available: https://fcc.web.cern.ch/Pages/default.aspx

[2] D. Tommasini *et al.*, "Status of the 16 T dipole development program for a future hadron collider," *IEEE Trans. Appl. Supercond.*, vol. 28, no. 3, Apr. 2018, Art. no. 4001305.

[3] EuroCirCol WP5 members, "16 T dipole design options input parameters and evaluation criteria," CERN, Geneva, Tech. Rep., 2015. [Online]. Available: https://indico.cern.ch/event/441684/

[4] V. Marinozzi *et al.*, "Conceptual design of a 16 T cos-θ bending dipole for the future circular collider," *IEEE Trans. Appl. Supercond.*, vol. 28, no. 3, Apr. 2018, Art. no. 4004205.

[5] C. Lorin, D. Durante, and M. Segreti, "Eurocircol 16 T block-coils dipole option for the future circular collider," *IEEE Trans. Appl. Supercond.*, vol. 27, no. 4, Jun. 2017, Art. no. 4001405.

[6] F. Toral, J. Munilla, and T. Salmi, "Magnetic and mechanical design of a 16 T common coil dipole for an FCC," *IEEE Trans. Appl. Supercond.*, vol. 28, no. 3, Apr. 2018, Art. no. 4004305.

[7] B. Auchmann *et al.*, "Electromechanical design of a 16-T CCT twin-aperture dipole for FCC," *IEEE Trans. Appl. Supercond.*, vol. 28, no. 3, Apr. 2018, Art. no. 4000705.

[8] M. Prioli, B. Auchmann, L. Bortot, M. Maciejewski, T. Salmi, and A. P. Verweij, "Conceptual design of the FCC-hh dipole circuits with integrated CLIQ protection system," *IEEE Trans. Appl. Supercond.*, 2019.

[9] T. Salmi *et al.*, "Quench protection analysis integrated in the design of dipoles for the future circular collider," *Phys. Rev. Accel. Beams*, vol. 20, no. 3, 2017, Art. no. 032401.

[10] F. Rodriguez-Mateos and F. Sonnemann, "Quench heater studies for the LHC magnets," in *Proc. Part. Accel. Conf.*, 2001, vol. 5, pp. 3451–3453.

[11] E. Ravaioli, "CLIQ," Ph.D. dissertation, University of Twente, Enschede, 2015. [Online]. Available: http://doc.utwente.nl/96069/

[12] E. Ravaioli, V. I. Datskov, C. Giloux, G. Kirby, H. H. J. ten Kate, and A. P. Verweij, "New, coupling loss induced, quench protection system for superconducting accelerator magnets," *IEEE Trans. Appl. Supercond.*, vol. 24, no. 3, Jun. 2014, Art. no. 0500905.

[13] M. Prioli and T. Salmi, "Quench protection studies for the FCC 16 T Nb3Sn dipoles developed within EuroCirCol," CERN Document Server (CDS), Tech. Rep., Sep. 2018.

[14] T. Salmi, M. Prioli, A. Stenvall, and A. P. Verweij, "Quench protection of the 16 T Nb$_3$ Sn dipole magnets designed for the future circular collider," *IEEE Trans. Appl. Supercond.*, vol. 29, no. 5, Aug. 2019, Art. no. 4700905.

[15] M. N. Wilson, *Superconducting Magnets*. New York, NY, USA: Clarendon Press–Oxford University Press, 1983.

[16] A. Verweij, "Electrodynamics of superconducting cables in accelerator magnets," Ph.D. dissertation, University of Twente, 1995. [Online]. Available: http://cds.cern.ch/record/292595/files/Thesis-1995-Verweij.pdf

[17] STEAM Website. Accessed: Oct. 1, 2019. [Online]. Available: https://cern.ch/steam?

[18] L. Bortot *et al.*, "A 2-D finite-element model for electrothermal transients in accelerator magnets," *IEEE Trans. Magn.*, vol. 54, no. 3, Mar. 2018, Art. no. 7000404.

[19] L. Bortot, "A consistent simulation of electrothermal transients in accelerator circuits," *IEEE Trans. Appl. Supercond.*, vol. 27, no. 4, Jun. 2017, Art. no. 4001305.

[20] I. C. Garcia *et al.*, "Optimized field/circuit coupling for the simulation of quenches in superconducting magnets," *IEEE J. Multiscale Multiphys. Comput. Techn.*, vol. 2, pp. 97–104, May 2017.

[21] L. Bortot *et al.*, "STEAM: A hierarchical cosimulation framework for superconducting accelerator magnet circuits," *IEEE Trans. Appl. Supercond.*, vol. 28, no. 3, Apr. 2018, Art. no. 4900706.

[22] COMSOL Multiphysics v. 5.3a *COMSOL Multiphysics v. 5.3a*. Stockholm, Sweden: COMSOL AB. [Online]. Available: https://www.comsol.com

[23] B. Bordini, M. Dhalle, and C. Senatore, "Specifications for conductors and proposed conductor configurations," CERN, Geneva, Tech. Rep., 2018. [Online]. Available: https://fcc.web.cern.ch/eurocircol/Documents/WP5/Milestone%20and%20Deli%verables/M5.3/EuroCirCol-1802280930-P2-WP5-M5-3_V0100.pdf

[24] E. Ravaioli, B. Auchmann, M. Maciejewski, H. ten Kate, and A. Verweij, "Lumped-element dynamic electro-thermal model of a superconducting magnet," *Cryogenics*, vol. 80, pp. 346–356, 2016.

[25] T. Salmi *et al.*, "Suitability of different quench protection methods for a 16 T block-type Nb$_3$Sn accelerator dipole magnet," *IEEE Trans. Appl. Supercond.*, vol. 27, no. 4, Jun. 2017, Art. no. 4702305.

[26] "ANSYS Mechanical v. 17.2." [Online]. Available: https://www.ansys.com

[27] J. Zhao *et al.*, "Mechanical stress analysis during a quench in CLIQ protected 16 T dipole magnets designed for the future circular collider," *Phys. C Supercond. Appl.*, vol. 550, pp. 27–34, 2018.

[28] M. Maciejewski *et al.*, "Coupling of magnetothermal and mechanical superconducting magnet models by means of mesh-based interpolation," *IEEE Trans. Appl. Supercond.*, vol. 28, no. 3, Apr. 2018, Art. no. 4900905.

[29] Fraunhofer SCAI, *MpCCI Coupling Environment 4.5*. [Online]. Available: https://www.mpcci.de

[30] G. Kirby *et al.*, "Thermal contraction of future magnet materials at cryogenic temperatures," CERN, Geneva, Tech. Rep. 1576936, 2016. [Online]. Available: https://edms.cern.ch/document/1576936/1